



ISSN 0975-413X
CODEN (USA): PCHHAX

Der Pharma Chemica, 2016, 8(2):488-492
(<http://derpharmachemica.com/archive.html>)

Effect of aluminium substitution in porous tin dioxide nanoparticles

S. Blessi, M. Maria Lumina Sonia, Bibi Francis and S. Pauline*

Department of Physics, Loyola College, University of Madras(India)

ABSTRACT

Mesoporous Tin dioxide (SnO_2) with varying weight % of Aluminium was prepared using hydrothermal method and was characterized by various techniques such as X- Ray Diffraction, FTIR, BET-surface area, pore size distribution and FESEM with EDAX. Analytical studies demonstrated that the as prepared SnO_2 is in tetragonal rutile phase and the crystallite size was found to decrease with the Al substitution. It was also observed that the Al substitution increases the BET surface area and the pore radius was found to decrease.

Keywords: Mesoporous, SnO_2 , surface area

INTRODUCTION

Tin Oxide (SnO_2), a functional wide band gap (3.6 eV) n- type semiconductor has been extensively studied due to its properties such as high degree of transparency in the visible spectrum, strong physical and chemical interaction with adsorbed species, low operating temperature and strong thermal stability in air (up to 500 °C). SnO_2 crystallizes with the rutile structure and has a tetragonal unit cell with $P4_2/mnm$ space group. SnO_2 has been extensively studied for transparent conductive electrodes [7], anodes for lithium ion batteries [4,12], dye - sensitized solar cells [13] and chemical gas sensors [9,10]. Metal doping of SnO_2 can improve the catalytic, electronic and electrochemical properties of the material. In particular the substitution of Sn^{4+} by Al^{3+} ions in the SnO_2 creates oxygen vacancies due to the charge imbalance thus generating free electrons in the conduction band. For the past decade porous materials have attracted remarkable attention since materials of this type exhibit unique physical and chemical properties different from the bulk. Porous materials with pore size of 2–50 nm are known as mesoporous materials [14] and are expected to have superior properties owing to their higher pore volume and extremely high surface area. Hence researchers are trying to develop mesostructured material with high specific surface area and ordered porous structure which makes them critically important for applications in gas sensors, solar cells and in drug delivery carriers. A variety of techniques have been reported to synthesize porous tin oxide materials, such as hard templating [15] or soft templating [8], hydrothermal [1], sol-gel [4], microwave assisted [5], molten salt [13], etc.

In the present study we demonstrate the synthesis of mesoporous SnO_2 with the Al (1%, 3% and 5%) substitution by simple hydrothermal method using cationic surfactant CTAB as template and Urea as counter ions. The materials were characterized by several techniques such as XRD, FESEM, FTIR, BET (Brauerer-Emmett-Teller) surface area and BJH (Barrett-Joyner-Halenda) pore size distribution.

MATERIALS AND METHODS

The chemical reagents used were hydrated Tin chloride ($\text{SnCl}_4 \cdot 5\text{H}_2\text{O}$) from Sigma, Aluminium Trichloride Hexahydrate ($\text{AlCl}_3 \cdot 6\text{H}_2\text{O}$), Cetyltrimethyl ammonium bromide(CTAB) ($\text{C}_{16}\text{H}_{33}\text{N}((\text{CH}_3)_3\text{Br})$), Urea ($\text{NH}_2)_2\text{CO}$ and ethanol($\text{C}_2\text{H}_5\text{OH}$). All chemicals used were as received without any further purification.

In a typical synthesis, $\text{SnCl}_4 \cdot 5\text{H}_2\text{O}$ was dissolved in a certain amount of deionised water to prepare 0.1M solution. CTAB was then added to the solution under constant stirring for 1 hour. After the dissolution of CTAB, urea was added dropwise to adjust the pH of the solution to 8. The solution was stirred for another one hour and then transferred to an autoclave for hydrothermal treatment at 100°C for desired time. The products were centrifuged and washed several times to remove Cl^- ions from the precipitate. Resulting products were dried at 80°C and then calcined at 600°C for 2 hours. Al doped SnO_2 was prepared by the same method with the addition of proper wt % (1,3 and 5) of $\text{AlCl}_3 \cdot 6\text{H}_2\text{O}$ to the 0.1 M solution of main precursor.

2.2 Characterization techniques

The X-ray diffraction (XRD) patterns of the as prepared pure and Al doped SnO_2 (1%,3%,5%) were studied using a Phillip PW 1800 X-ray diffractometer with $\text{Cu K}\alpha$ radiation of wavelength 1.5405\AA . Field emission scanning electron microscopy (FESEM) was carried out using CARL ZEISS SUPRA 55 operated at an accelerating voltage of 20 kV. FTIR of the samples were recorded using JASCO 4100, operating in the range of 4000 to 400 cm^{-1} . BET (Brunauer-Emmett-Teller) surface area and BJH (Barrett-Joyner-Halenda) pore size distribution was measured by Micromeritics ASAP 2020 porosimeter.

RESULTS AND DISCUSSION

3.1 Structural studies

The powder XRD pattern of the pure and Al doped SnO_2 are shown in Figure 1. The peaks in XRD pattern shows that it is crystalline and the position of the peaks reveal that the samples are in tetragonal rutile phase (JCPDS card no:41 - 1445, space group $\text{P}4_2/\text{mm}$, $a_0 = 4.738\text{\AA}$, $c_0 = 3.187\text{\AA}$). There was no shift in the diffraction peaks of Al doped SnO_2 and no impurity phase correlated with Al was observed. The absence of any additional peak in the XRD pattern with different % of Al doping only indicates that the substitution does not distort the original structure. The average grain size of all the samples were calculated using Scherrer equation and are shown in Table 1. As seen from Table 1, it is evident that the Al doping with the concentrations 1%,3%, and 5% had little effect on the crystallite sizes. The lattice parameters were calculated using XRDA software and are listed in Table 1. The values are very close to standard value for bulk SnO_2 .

Samples	Crystallite size (nm)	a (Å)	c (Å)	u=c/a
Pure SnO_2	39	4.731 ± 0.0022	3.1901 ± 0.0021	0.6740 ± 0.0005
Al 1% doped	34	4.7239 ± 0.0053	3.1714 ± 0.005	0.6714 ± 0.0012
Al 3% doped	33	4.7036 ± 0.0068	3.1879 ± 0.006	0.6778 ± 0.0013
Al 5% doped	32	4.7430 ± 0.0022	3.1722 ± 0.002	0.6688 ± 0.0005

Table 1. Lattice parameters of pure and doped SnO_2

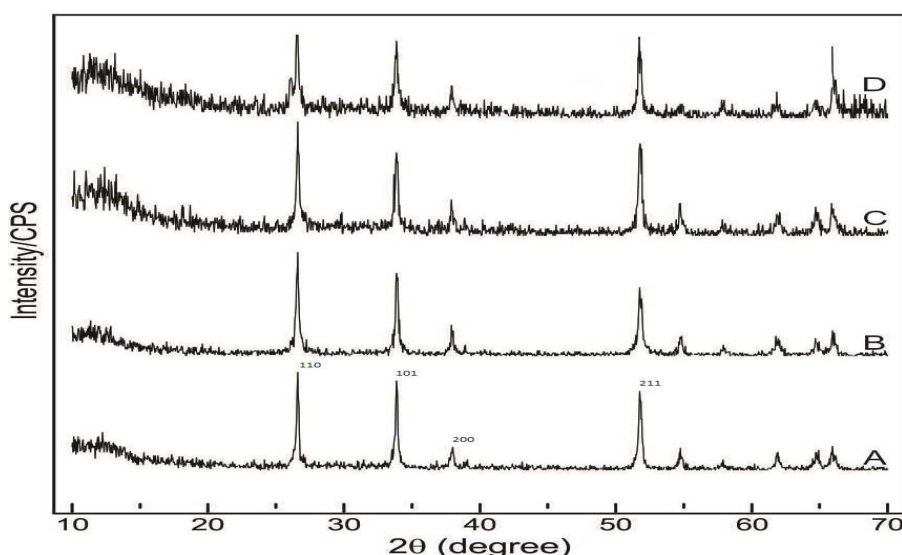


Figure 1. XRD Pattern of pure (A) and Al doped SnO_2 (B, C and D)

3.2 FTIR Studies

To complement the XRD analysis, FTIR spectroscopic measurements were performed for all the samples and are shown in Figure 2. Minimum transmittance on the wavelength range of $3400 - 3700\text{ cm}^{-1}$ is related to the O-H bond stretching vibrations of water molecule adsorbed. The bands around 1400 cm^{-1} was assigned to the NH deformation

of ammonia and NH stretching vibrations from decomposition of urea which was used as counter ions during the synthesis. Furthermore peaks observed at 1024 cm^{-1} and 625 cm^{-1} are assigned to the fundamental vibrations of Sn-O which correspond to the asymmetric Sn-O-Sn stretching mode

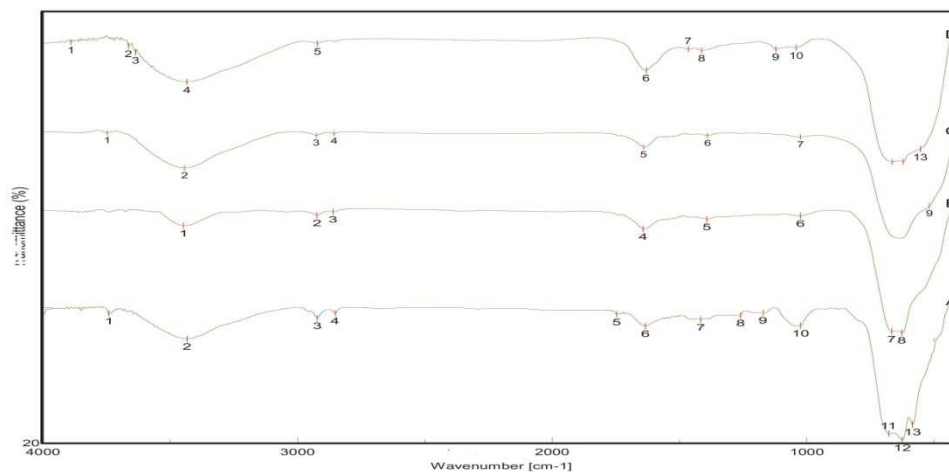


Figure 2. FTIR images of pure (A) and Al doped SnO_2 (B, C and D)

3.3 Morphological study: FESEM

To understand the morphology of the porous Al doped SnO_2 , FESEM was carried out and are shown in Figure 3. It is observed from the micrographs, that the particles are spherical in shape and tend to agglomerate leaving some pores in between. In order to check whether the template molecules are completely removed during the calcination process, the samples were analyzed with FESEM - EDAX (Figure 4). As seen from the spectrum, the samples show only the peaks relating to Sn, O and Al and no other impurities could be detected. It is evident from these spectrum that the peak intensity of O is much lesser in Figure 3b, 3c, and 3d compared to Figure 3a, which is attributed to the fact the addition of Al creates more oxygen vacancies since Sn^{4+} ions are replaced by Al^{3+} ions. This makes the material more n-type semiconductors.

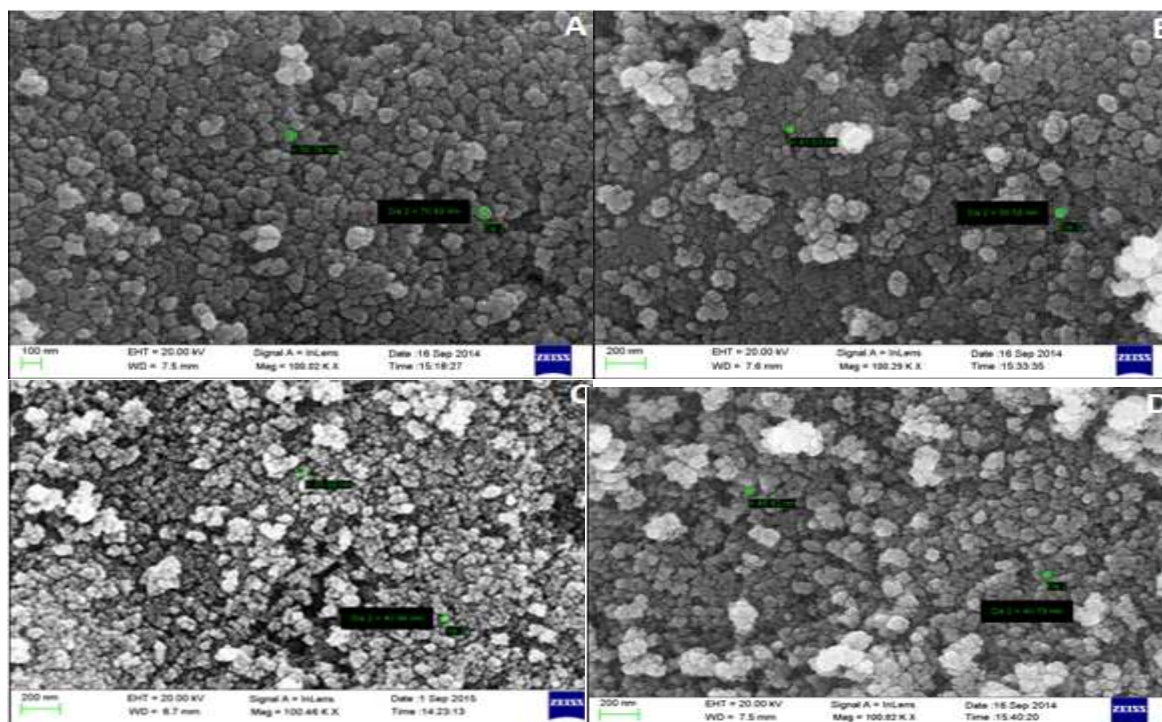


Figure 3. FESEM images of pure (A) and Al doped SnO_2 (B,C,D)

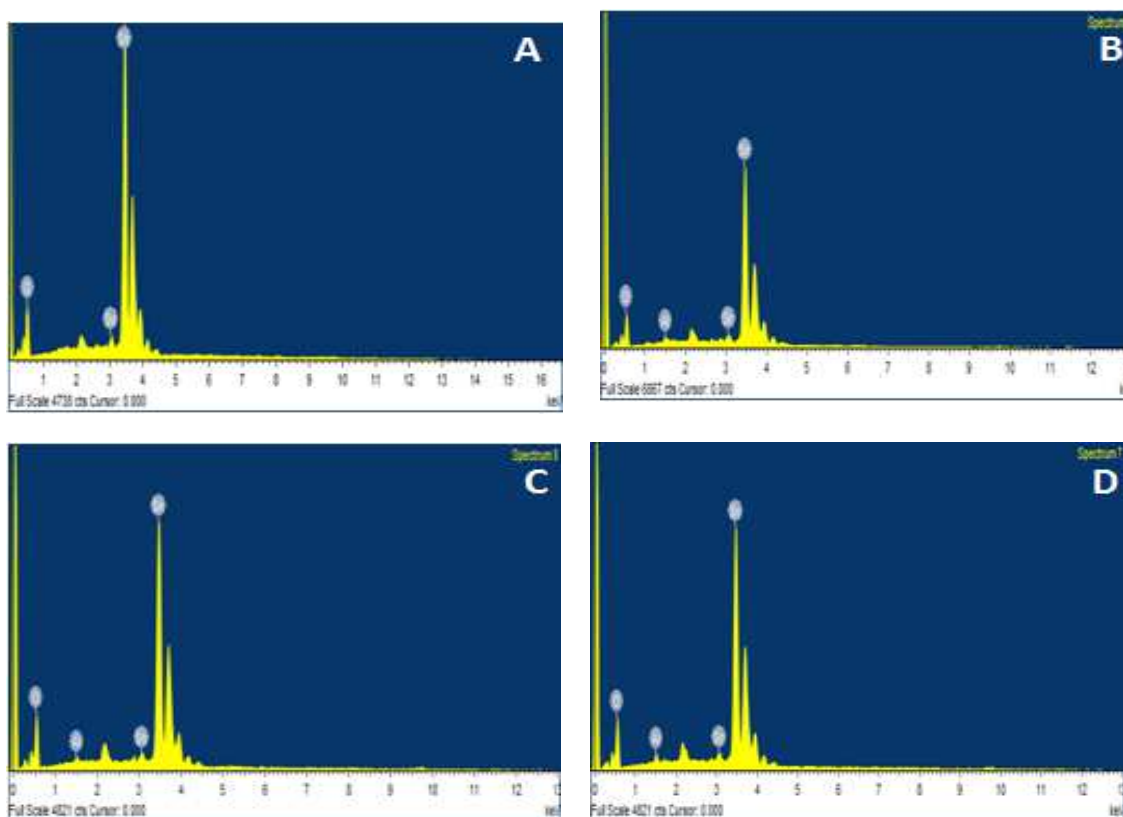
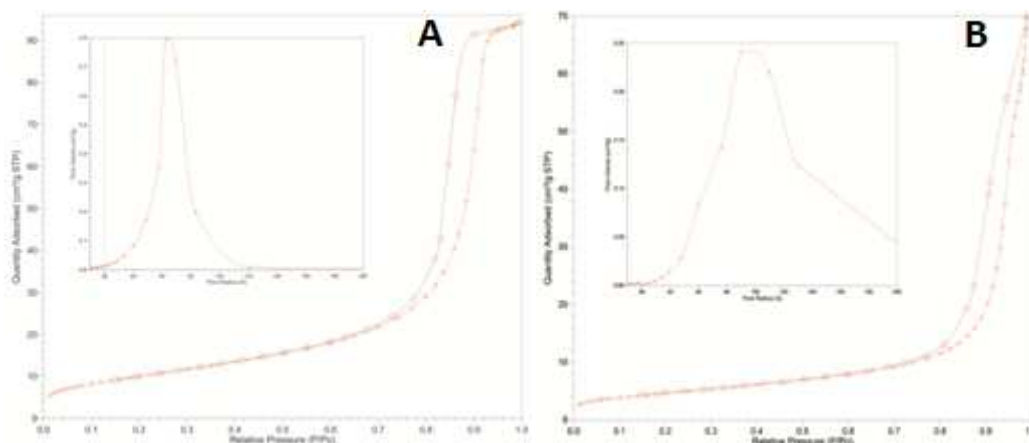


Figure 4. EDAX Spectrum of pure (A) and Al doped SnO₂ (B,C,D)

3.4 N₂ adsorption-desorption isotherm

The porous structure was characterized by N₂ adsorption-desorption and the BET surface area of the as prepared samples are presented in Figure 4 and the parameters are summarized in Table 2. As shown in Figure 4, the nitrogen adsorption-desorption isotherms of pure and Al doped SnO₂ show that they are of type IV with a distinct hysteresis loop observed in the range of 0.6 - 1 p/p₀ according to IUPAC classification indicative of porous structures. Hysteresis loop observed in the plot is associated with the filling and emptying of mesopores by capillary condensation. Pore size distribution was then determined by Barrett-Joyner-Halenda (BJH) method and the plots are shown in inset of Figure 4. The BJH plot clearly shows that pores of average size 2 - 20 nm are dominant in the resultant product. It is clear from Table 2 that on incorporation of Al³⁺, the particle size and the pore radius reduces suggesting that the dopant influences the grain growth and the porosity of pure SnO₂ material. The reduction in particle size is gradual with dopant concentration which is in agreement with BET surface area results. The specific surface area of Al-SnO₂ (5%) was evaluated to be 42 m²/g based on the BET result and this surface area is comparatively higher than those of the reported mesoporous SnO₂ synthesized by chemical coprecipitation methods [8,16]. This high surface area and the mesoporous nature of the material is expected to be beneficial for absorbing gas molecules.



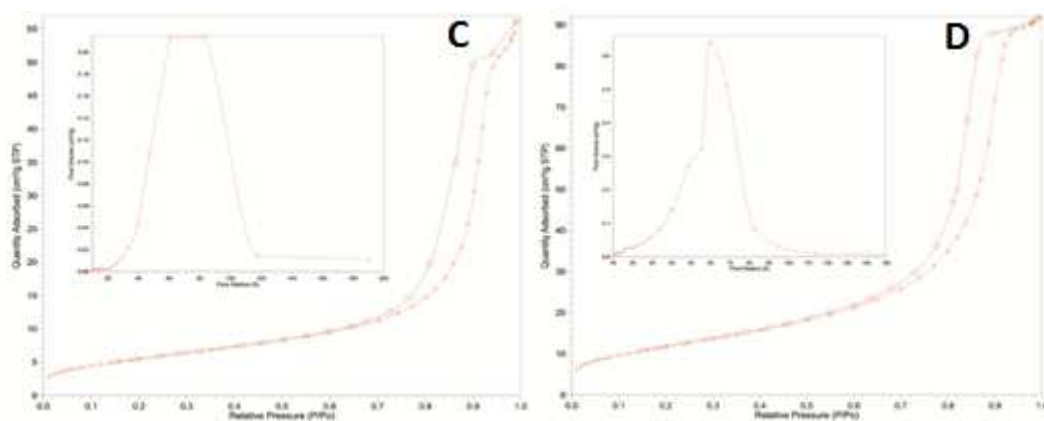
Figure 4. N₂ adsorption - desorption isotherms

Table 2.

Sample	BET Surface Area (m ² /g)	BJH Pore Size (nm)	BJH Pore Volume (cm ³ /g)	Crystallite Size (nm)
SnO ₂	15	10.6	0.080	39
Al-SnO ₂ (1%)	16	9.8	0.107	34
Al-SnO ₂ (3%)	19	6.3	0.086	33
Al-SnO ₂ (5%)	42	4.8	0.142	32

CONCLUSION

In the present work, pure and varying percents (1, 3, and 5) of Al doped mesoporous SnO₂ have been successfully synthesized using simple hydrothermal method. The structural investigation carried out using the X-ray Diffraction technique indicated the tetragonal rutile phase of the as prepared sample and the average crystallite size was calculated for the high intensity peak. Surface area and the porosity studies confirmed the mesoporous nature of the host material. It is noteworthy to mention that doping of SnO₂ with Al indicated an increase in the surface area and a corresponding decrease in the pore radius. The maximum surface area was observed in 5% doping of Al. Morphology of the as prepared particles were discussed with FESEM and EDAX pattern which confirmed the oxygen trapping in all the doped samples.

Acknowledgement

The author wishes to thank the university of Madras, Sathyabama university and Indian Institute of Technology Madras for the facilities utilized in the work

REFERENCES

- [1] Farrukh, B. T. Heng and Adnan, *Turk J. Chem.*, **2010**, 84, 537 – 550
- [2] Ji Eun Ko, Bob Jin Kwan, Hyun Jung, *Journal of Physics and Chemistry of Solids*, **2010**, 71, 658 - 662
- [3] Luhua Jiang, Gongquan Sun, Zhenhua Zhou, *J phy chem B*, **2005**, 109, 8774 - 8778
- [4] Alok kumar Roy, Ly Tuan Auh, Jihyeon Gim, *Electrochimica Acta*, **2013**, 109, 461-467
- [5] Suraj K. Tripathy, Amrita Mishra, Sandeep kumar Jha, *J Mater Sci.*, **2013** doi 10.1007/3 10854 - 013- 1062 - 0
- [6] N Kumari, A Ghosh, S Tewari and A Bhattacharjee, *Indian J Phys*, **2013** doi 10.1007/s 12648 - 013 - 0387 - 0
- [7] Yu - Zhou Zhang, Huan Pang, Yanqiu San, *Int. J Electrochem. Sci*, **2013**, 8, 3371 - 3378
- [8] Muhammad Akhyar Farrukh, P Tan, *Turk J. Chem.*, **2012**, 36, 303-314
- [9] Thorsten Wagner, Claus Kohl, Michael Froba, *Sensors*, **2006**, 6, 318 - 323
- [10] Xinzhen Wang, Song Qui, *European J Inorganic Chem*, **2014**, 5, 863-869
- [11] Konda Shiva & M. S. R. N. Kiran & U. Ramamurthy, *J Solid State Electrochem*, **2012**, 16, 3643 - 3649
- [12] Ameer Azam Sami, S Habib Numan, A Salah Faheem Ahmed, *International Journal of Nanomedicine*, **2013**, 8, 3875-3882
- [13] Peining Zhu, M. V. Reddy Yongzhi Wu, *Royal Society of Chem*, **2012**,
- [14] Huihua Li, Fanli Meng, Jinyun Liu, *Sensors and Actuators B*, **2012**, 166-167, 519 - 525
- [15] Juong Kuk Shon, Soo Sung Kong, Yoon Sung Kim, *Microporous and Mesoporous materials* **2009**, 120, 441-446
- [16] Shoichi Tekanaka Ryoji Takahashi, *Microporous and Mesoporous materials*, **2003**, 59, 121 - 131